Resonant Modes in Shielded Cylindrical Ferrite and Single-Crystal Dielectric Resonators

JERZY KRUPKA

Abstract—**The Galerkin–Rayleigh–Ritz method is applied for computing the first few lowest resonant frequencies of cylindrical anisotropic resonators in a cylindrical cavity. The resonators are allowed to have gyromagnetic and uniaxial dielectric anisotropy with respect to the z axis of the cylinder. Results of computations of the resonant frequencies are compared with exact solutions for many simple resonant structures and with results of experiments for more complicated structures. A new method of measuring permeability tensor components is presented. The method utilizes two parallel-plate cylindrical resonators operating in the $HE_{111}^{\pm}$ and H_{011} modes. A method of measuring permittivity tensor components of single crystals is proposed using one parallel-plate cylindrical resonator operating in two different modes.**

I. Introduction

In this paper the resonant modes of cylindrical anisotropic resonators in cylindrical cavities are discussed. The geometry under study is illustrated schematically in Fig. 1. This configuration is important for such applications as the precise measurement of permeability or permittivity tensor components of low-loss anisotropic materials and the design of circulators containing a ferrite cylinder. It is assumed that the resonator is made of a lossless medium characterized by the following permittivity and permeability tensors:

$$\overleftrightarrow{\epsilon} = \begin{bmatrix} \epsilon & 0 & 0 \\ 0 & \epsilon & 0 \\ 0 & 0 & \epsilon_z \end{bmatrix} \tag{1}$$

$$\overleftrightarrow{\mu} = \begin{bmatrix} \mu & -j\kappa & 0 \\ j\kappa & \mu & 0 \\ 0 & 0 & \mu_z \end{bmatrix}. \tag{2}$$

II. Theory

In order to determine the resonant frequencies of the resonant system shown in Fig. 1, we shall solve the following eigenvalue problem:

$$L\vec{\Phi} = j\omega M\vec{\Phi}$$

$$\vec{n}\times\vec{E} = 0 \qquad \text{on } S \tag{3}$$

Manuscript received October 19, 1987; revised October 25, 1988.

The author is with the Instytut Mikroelektroniki i Optoelektroniki Politechniki Warszawskiej, 00-662 Warszawa, Koszykowa 75, Poland.

IEEE Log Number 8826037.

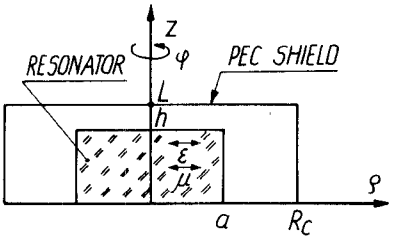

Fig. 1. Cylindrical anisotropic resonator in a cylindrical cavity.

where

$$L = \begin{bmatrix} 0 & \text{curl} \\ \text{curl} & 0 \end{bmatrix} \qquad M = \begin{bmatrix} \epsilon_0\overleftrightarrow{\epsilon} & 0 \\ 0 & -\mu_0\overleftrightarrow{\mu} \end{bmatrix}$$

$$\vec{\Phi} = \begin{bmatrix} \vec{E} \\ \vec{H} \end{bmatrix}.$$

Here $\vec{E}$ and $\vec{H}$ are the electric and magnetic fields inside the cavity, and S is the surface of the cavity. A rigorous solution to problem (3) obtained by means of the Galerkin–Rayleigh–Ritz method (G–R–R method) [1], [2] using an empty cavity (having the same boundary S) serves as a basis. The solution to the original problem (3) is taken to be

$$\vec{E} = \sum_{n=1}^{N} \alpha_n^E \vec{E}_n^0 + \sum_{n'=1}^{N'} \alpha_{n'}^F \vec{F}_{n'}^0$$

$$\vec{H} = \sum_{n=1}^{N} \alpha_n^H \vec{H}_n^0 + \sum_{n''=1}^{N''} \alpha_{n''}^G \vec{G}_{n''}^0 \tag{4}$$

where $\alpha_n^E, \alpha_n^H, \alpha_{n'}^F, \alpha_{n''}^G$ are field expansion coefficients to be determined, $\vec{E}_n^0, \vec{H}_n^0$ are rotational electric and magnetic basis functions corresponding to the electric and magnetic fields of an empty cavity having boundary S, and $\vec{F}_{n'}^0, \vec{G}_{n''}^0$ are potential electric and magnetic basis functions of an empty cavity having boundary S. Full expressions for the basis functions of a cylindrical cavity are given in the Appendix.

Substituting (4) into (3), forming inner products with each of the basis functions, and finally eliminating $[\alpha^H]$, $[\alpha^F]$, and $[\alpha^G]$ from the system of linear equations, one obtains [1], [2]

$$\sum_{n=1}^{N} \left(A_{kn} - \delta_{kn}\omega^{-2}\right)\alpha_n^E = 0, \qquad k = 1,2,\cdots,N \tag{5}$$

where

$$[A] = [\Omega]^{-1}[m^H][\Omega]^{-1}[m^E]$$

$$[m^E] = [m^{EE}] - [m^{EF}][m^{FF}]^{-1}[m^{FE}]$$

$$[m^H] = [m^{HH}] - [m^{HG}][m^{GG}]^{-1}[m^{GH}]$$

$$m_{kn}^{EE} = \langle \epsilon_0 \overleftrightarrow{\epsilon} \vec{E}_n^0, \vec{E}_k^0 \rangle,\ m_{kn}^{EE} = \langle \epsilon_0 \overleftrightarrow{\epsilon} \vec{F}_n^0, \vec{E}_k^0 \rangle$$

$$m_{kn}^{HH} = \langle \mu_0 \overleftrightarrow{\mu} \vec{H}_n^0, \vec{H}_k^0 \rangle,\ m_{kn}^{HG} = \langle \mu_0 \overleftrightarrow{\mu} \vec{G}_n^0, \vec{H}_k^0 \rangle.$$

(The elements of the remaining matrices $[m^{FF}]$, $[m^{FE}]$, $[m^{GG}]$, and $[m^{GH}]$ are defined in the same way.) In addition,

$$[\Omega] = \begin{bmatrix} \omega_1^0 & 0 & \cdots & 0 \\ 0 & \omega_2^0 & \cdots & 0 \\ \cdots & & \cdots & \cdots \\ 0 & 0 & & \omega_N^0 \end{bmatrix}$$

$$\langle f, g \rangle \underset{df}{=} \int_v fg^* dv \quad \text{and} \quad \delta_{nn} = \text{Kronecker delta}.$$

The system of equations (5) has nontrivial solutions for ω^{-2} values that are eigenvalues of the matrix $[A]$. If a complete set of basis functions is used, an exact solution to the original problem can be obtained, at least in principle, by letting N, N', and $N'' \to \infty$. To take advantage of the rotational symmetry of the resonant system we can consider modes having different ϕ dependences separately. This reduces the size of the matrix eigenvalue problem and allows easier mode identification.

III. Computations

Standard Fortran routines for matrix inversion and computations of matrix eigenvalues have been applied in the computer program used for the numerical solution of the problem (5). Integrals containing products of Bessel functions and their derivatives have been computed numerically (Gaussian quadrature) for ϕ-dependent modes and analytically for ϕ-independent modes. As the first example of our computations we consider a cavity completely filled with a gyromagnetic medium. The following parameters have been taken for the computations: $L = h = a = R_c$, $\epsilon_z = \epsilon$, and $\mu_z = \mu$. The $\vec{H}_{mnp}^0$ and $\vec{G}_{mnp}^0$ functions have been taken as a basis. For each m and p we took the basis with $n = 1, 2, \cdots, 13$. The size of matrix $[A]$, however, was 26×26 since it depends on the total number of rotational functions (13 for the electric-type and 13 for the magnetic-type functions). The results of computations of the normalized resonant frequencies for the first few modes versus $|\kappa/\mu|$ values are presented in Figs. 2 and 3 (broken lines). For comparison, exact resonant frequency values are drawn (solid lines). The exact values were found as roots of the well-known transcendental equation derived by Kales [3]. Modes marked with a plus or minus superscript correspond to κ/μ ratios that are, respectively, positive or negative. Modes without a superscript show the same behavior for κ/μ both positive and negative. The convergence of the G–R–R method depends on the κ/μ value and the mode of interest. For $|\kappa/\mu| \leqslant 0.4$, differences between exact and approximate results are not greater than 0.2 percent for all modes considered in Figs. 2 and 3. For ϕ-dependent modes the convergence strongly depends on the sign of rotation or, what is equivalent, the sign of κ/μ. For all modes with a minus superscript the convergence is worst than for modes with the opposite sign. This is presented in Table I for the $H_{111}^{\pm}$ modes. For the HE_{111}^{-} mode the poorest convergence occurs for $\kappa/\mu = -0.8$ (1.05 percent error) while for $\kappa/\mu = -1.0$ it improves (0.8 percent error). For the HE_{111}^{+} mode the convergence is excellent (0.05 percent error) for all κ/μ values considered in Table I. For modes with rotational symmetry the convergence depends on the $|\kappa/\mu|$ value and the mode of interest. For the H_{011} mode the poorest convergence occurs for $|\kappa/\mu| = 0.7$, while for all z-independent modes (Fig. 3) this occurs for $|\kappa/\mu| \Rightarrow 1$.

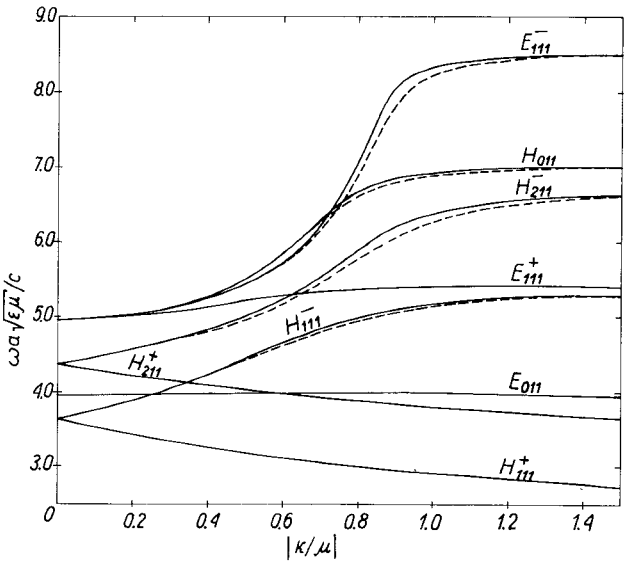

Fig. 2. Normalized resonant frequencies for z-dependent modes of the cylindrical cavity completely filled with gyromagnetic medium versus $|\kappa/\mu|$ values. $L = h = a = R_c$, $\epsilon_z = \epsilon$, $\mu_z = \mu$. —— exact values; ---- approximate values obtained by means of the G–R–R method.

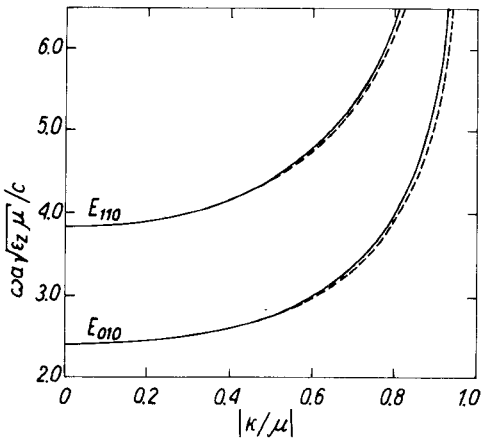

Fig. 3. Normalized resonant frequencies for z-independent modes of the cylindrical cavity completely filled with gyromagnetic medium versus $|\kappa/\mu|$ values $L = h$, $a = R_c$. —— exact values; ---- approximate values obtained by means of the G–R–R method.

TABLE I
NORMALIZED $HE_{111}^{\pm}$ MODE FREQUENCIES OF THE CYLINDRICAL CAVITY COMPLETELY FILLED WITH GYROMAGNETIC MEDIUM

Mode	HE_{111}^{-}					H_{111}	HE_{111}^{+}				
κ/μ / n_{max}	−1.0	−0.8	−0.6	−0.4	−0.2	0	0.2	0.4	0.6	0.8	1.0
3	4.9443	4.7625	4.5034	4.1929	3.8935	3.6414	3.4371	3.2714	3.1350	3.0213	2.9250
8	5.0353	4.9243	4.5950	4.2181	3.8967	3.6414	3.4380	3.2734	3.1379	3.0246	2.9285
13	5.0686	4.9590	4.6172	4.2243	3.8975	3.6414	3.4383	3.2740	3.1386	3.0254	2.9294
exact	5.1170	5.0118	4.6537	4.2345	3.8988	3.6414	3.4386	3.2749	3.1399	3.0268	2.9309

The frequencies are computed using a different number of basis functions (all basis functions are taken with subscripts $n=1,2,\cdots,n_{\max}$). $\omega a\sqrt{\epsilon\mu}/c$ values for $h=L=a=R_c$, $\mu=\mu_z$, and $\epsilon=\epsilon_z$.

TABLE II
NORMALIZED $HE_{111}^{\pm}$ MODE FREQUENCIES OF THE CYLINDRICAL GYROMAGNETIC RESONATOR IN A CYLINDRICAL CAVITY

Mode		HE_{111}^{-}					HE_{111}	HE_{111}^{+}		
	κ/μ / n_{max}	−1.0	−0.8	−0.6	−0.4	−0.2	0	0.2	0.5	1.0
$R_c=2a$	3	4.7770	4.8638	4.9743	4.7270	4.1876	3.8048	3.5289	3.2296	2.9010
	8	4.5933	4.6703	4.7608	4.6876	4.1821	3.8059	3.5303	3.2314	2.9046
	13	4.5957	4.6720	4.7615	4.6868	4.1834	3.8076	3.5327	3.2335	2.9073
$R_c=3a$	8	4.5943	4.6736	4.7647	4.6903	4.1795	3.8032	3.5275	3.2285	2.9013

The frequencies are computed using a different number of basis functions (all basis functions are taken with subscripts $n=1,2,\cdots,n_{\max}$). $\omega a\sqrt{\epsilon\mu}/c$ values for $h=L=a$, $\mu=\mu_z=1.0$, and $\epsilon=\epsilon_z=10$.

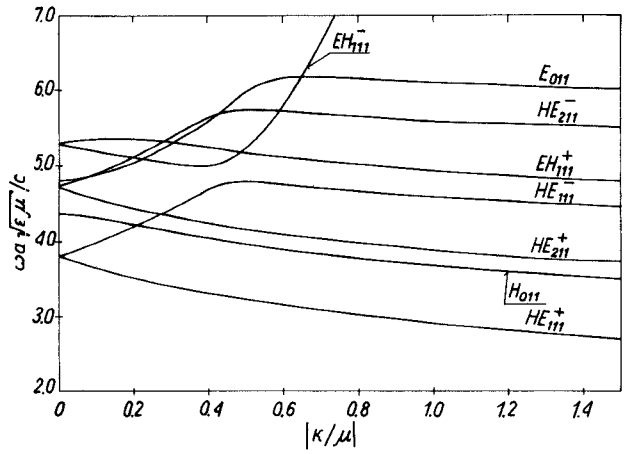

Fig. 4. Normalized resonant frequencies for interior modes of the cylindrical gyromagnetic resonator in a cylindrical cavity versus $|\kappa/\mu|$ values. $L=h=a$, $R_c\geq 2a$, $\epsilon_z=\epsilon=10$, $\mu_z=\mu=1$.

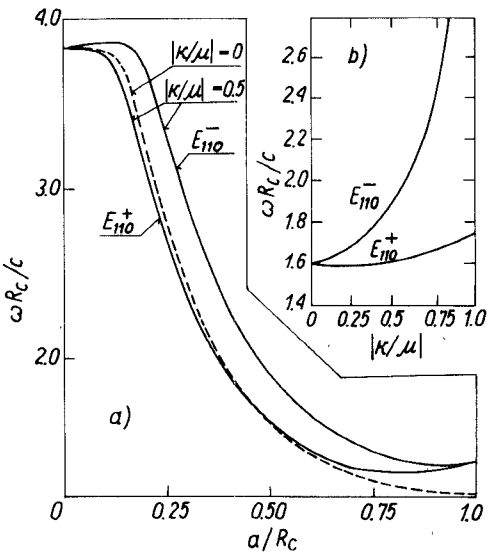

Fig. 5. (a) Normalized resonant frequencies for $E_{110}^{\pm}$ modes of the cylindrical gyromagnetic resonator versus a/R_c values, with $\epsilon_z=10$ and $\mu=1$. (b) Normalized resonant frequencies for $E_{110}^{\pm}$ modes of the cylindrical gyromagnetic resonator versus $|\kappa/\mu|$ values, with $\epsilon_z=10$, $\mu=1$, and $a/R_c=0.5$.

As a second example we consider a cavity containing a ferrite cylinder having the same height but a radius different from that of the cavity. The following parameters have been taken for computations: $L=h=a$, $R_c=2a$, $\epsilon=\epsilon_z=10$, and $\mu=\mu_z=1$. A basis taken for the computations is similar to that used in the first example but it additionally includes the electric basis functions $\vec{E}_{mnp}^{0}$ and $\vec{F}_{mnp}^{0}$ with $n=1,2,\cdots,13$. The results of computations of the normalized resonant frequencies for the first few interior modes are presented in Fig. 4. We notice that, as with dielectric resonators, we can divide all modes into two categories: the interior modes and the exterior ones. For the first category the energy stored in the electromagnetic field is predominantly concentrated in the gyromagnetic medium and, what is more important, it does not radiate outside the resonator in the absence of the lateral surface of the cavity (assuming that the flat surfaces are infinitely large). For the second category, in the absence of the lateral surface of the cavity, radiation of energy always takes place and the Q factor for these modes is low. The convergence of the G–R–R method for all interior modes considered in Fig. 4 seems to be better than for the completely filled cavity. The convergence for the $HE_{111}^{\pm}$ modes is presented in Table II. Normalized frequency values obtained with a different number of basis functions ($n_{\max}=8$ and $n_{\max}=13$) and for different radii of the cavity ($R_c=2a$ and $R_c=3a$) are consistent for all values considered in Table II. For the completely filled cavity, the differences between results obtained with $n_{\max}=8$ and $n_{\max}=13$ were much greater (Table I). For $R_c\geq 2a$ the resonant frequencies for all the interior modes considered in Fig. 4 do not depend on R_c. Hence the results shown in Fig. 4 are also valid for a parallel-plate gyromagnetic resonator having the same parameters.

We remark that for a gyromagnetic rod having the same height as the height of the cavity (or as the distance between plates for the parallel-plate resonator) the characteristic equation is also known [4], so exact solutions could have been obtained. We decided not to solve the above-mentioned equation (except for the z-independent modes, where it becomes relatively simple) since it is rather cumbersome.

In Fig. 5 the results of computations of the $E_{110}^{\pm}$ mode frequencies are presented versus the relative radius (a/R_c) of the sample (Fig. 5(a)) and versus $|\kappa/\mu|$ for fixed a/R_c value (Fig. 5(b)). For these modes we have also solved the transcendental equation [4], [5] to get its exact solutions. However the differences between the exact results (roots of the transcendental equation) and the approximate ones were too small to make them in the scale of Fig. 5.

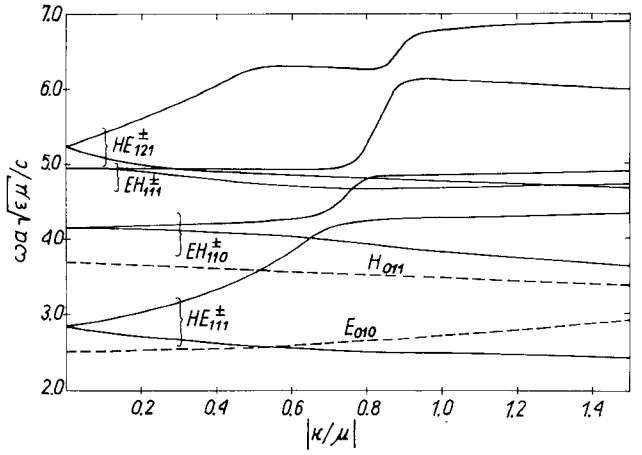

Fig. 6. Normalized resonant frequencies for the first few modes of the cylindrical gyromagnetic resonator in a cylindrical cavity versus $|\kappa/\mu|$ values. $h=a$, $R_c=2a$, $L=2h$, $\epsilon_z=\epsilon=10$, $\mu_z=\mu=1$.

Generally we can state that the convergence of the G–R–R method is worse for small a/R_c values. The resonant frequencies of the $E_{110}^{\pm}$ modes do not depend on L/R_c, ϵ, or μ_z but depend strongly on the a/R_c value. We also observe that mode splitting for these modes disappears for $a/R_c=1$ (this can also be seen in Fig. 3).

In Fig. 6 we present results of computations of the normalized resonant frequencies versus $|\kappa/\mu|$ for a resonant system for which exact solutions are not available. The following parameters have been taken for computations: $h=a$, $R_c=2a$, $L=2h$, $\epsilon=\epsilon_z=10$, $\mu=\mu_z=1$, $m=0$, and $m=1$. Subscripts n and p of the basis functions used for the above computations are presented schematically in Fig. 7.

As the next example we consider the influence of uniaxial magnetic and dielectric anisotropy on the resonant frequencies of different modes for a completely filled cavity and for a cavity having the same height but different radius from that of the anisotropic medium. For a cylindrical cavity completely filled with medium having uniaxial anisotropy (assuming that the anisotropy axis is parallel to the z axis of the cavity) the normalized resonant frequency values are given explicitly by the following expressions [6]:

$$\omega a\sqrt{\epsilon\mu}/c=\sqrt{u_{mn}^2\epsilon/\epsilon_z+(p\pi a/L)^2} \qquad \text{for } E_{mnp} \text{ modes} \tag{6}$$

$$\omega a\sqrt{\epsilon\mu}/c=\sqrt{(u'_{mn})^2\mu/\mu_z+(p\pi a/L)^2} \qquad \text{for } H_{mnp} \text{ modes} \tag{7}$$

where u_{mn} denotes the nth zero of the mth-order Bessel function, and u'_{mn} is the nth zero of the derivative of the mth-order Bessel function. It is seen that the H_{mnp} modes are independent of the dielectric anisotropy and the E_{mnp} modes are independent of the magnetic anisotropy. Hence, for a cylindrical cavity with dielectric uniaxial anisotropy, the G–R–R method leads to exact results for all H_{mnp} modes. The same is true for magnetic uniaxial anisotropy for all E_{mnp} modes. It is not so evident that the G–R–R method leads also to exact results for all modes of a cylindrical cavity completely filled with media having electric and/or magnetic uniaxial anisotropy. It can be proved that in this case the matrices $[m^E]$ and $[m^H]$ become diagonal and expressions (6) and (7) can be derived directly from their diagonal elements.

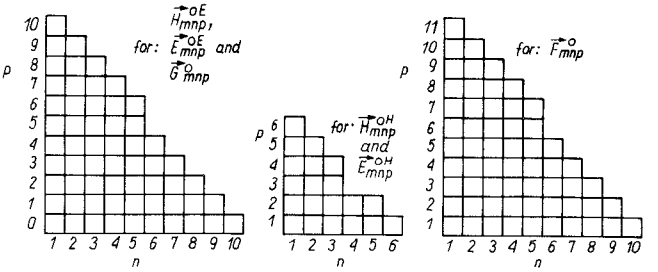

Fig. 7. Subscripts of basis functions used for computations of frequencies in Fig. 6

As for gyromagnetic resonators, we have used only the G–R–R method for computations of the resonant frequencies of a cavity partially filled with media having dielectric uniaxial anisotropy. The results of computations of normalized resonant frequencies for the first four interior modes of the resonant system with parameters $L=h=a$, $R_c=2a$, $\mu=\mu_z=1$, and $\kappa=0$ are shown in Fig. 8. The $\vec{E}_{mnp}^{o}$ and $\vec{F}_{mnp}^{o}$ functions with $n=1,2,\cdots,8$ have been taken as a basis. The results shown in Fig. 8 are also valid for $R_c\Rightarrow\infty$ for the same reason as for interior modes of the gyromagnetic resonators considered earlier. We observe in Fig. 8 that only the H_{011} mode (generally all H_{0np} modes) does not depend on the ϵ_z value. This is clear since for $a<R_c$ all ϕ-dependent modes are hybrid so they have the electric field component parallel to the axis of anisotropy.

IV. Experiments

We employed two cylindrical parallel-plate resonators made of the same material (yttrium-iron-garnet ferrite) but having different dimensions for measurements of all permeability tensor components versus external field intensity. The dimensions of the resonators were chosen in such a way as to get approximately the same frequencies for the HE_{111} mode of the smaller resonator and the H_{011} mode of the greater one for a demagnetized sample. (We used two resonators to minimize errors caused by the dependence of the tensor components on frequency.) As the first step of our experiment the surface resistance of the metal plates was measured using two low-loss dielectric H_{011} mode resonators made of the same material and having the same resonant frequencies but different aspect ratios [7]. As the second step, the permittivity, the scalar permeability, and the electric and magnetic loss tangents of the greater ferrite resonator were measured by means of Courtney's method [8]. Then the resonant frequencies and unloaded Q factors of the HE_{111}^{-}, HE_{111}^{+}, and H_{011} modes were measured versus magnetic field intensity. The results of the experiments are presented in Fig. 9. For each value of external field intensity the real parts of the permeability

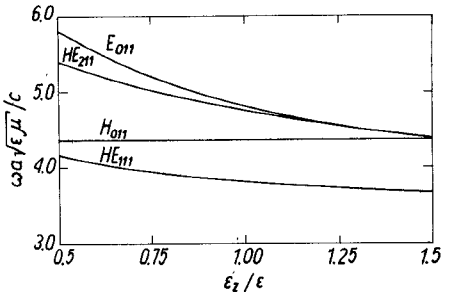

Fig. 8. Normalized resonant frequencies for interior modes of the cylindrical resonator, having dielectric uniaxial anisotropy, in a cylindrical cavity versus ϵ_z/ϵ values. $L=h=a$, $R_c \geq 2a$, $\epsilon=10$.

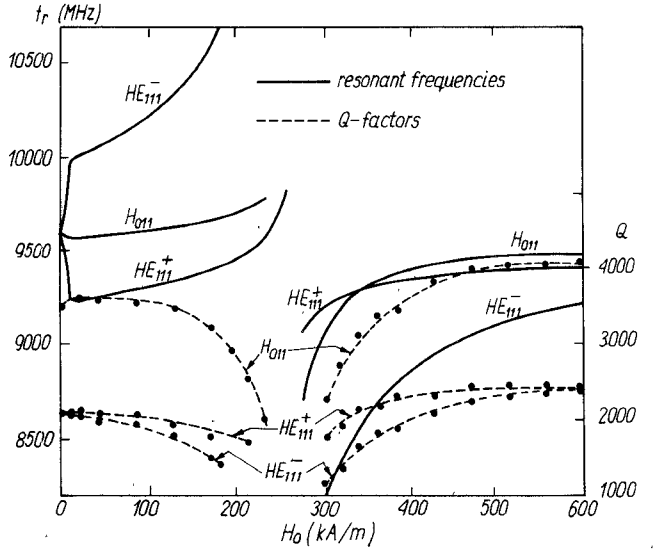

Fig. 9. Resonant frequencies and unloaded Q factors of the cylindrical parallel-plate yttrium-iron-garnet resonators versus external magnetic field intensity. ——— results of experiments for the $HE_{111}^{\pm}$ mode resonator having $h=7.02$ mm, $a=3.52$ mm, $\epsilon=14.15$, and $\tan\delta_\epsilon=1.9\times10^{-4}$. – – – – results of experiments for the H_{011} mode resonator having $h=8.38$ mm, $a=4.19$ mm, $\epsilon=14.15$, and $\tan\delta_\epsilon=1.9\times10^{-4}$.

tensor components were found by an iterative solution of the following system of equations:

$$f_r^- - f_r^+ = F_1(\mu, \kappa, \mu_z) \tag{8}$$

$$f_r^- + f_r^+ = F_2(\mu, \kappa, \mu_z) \tag{9}$$

$$f_r^0 = F_3(\mu, \kappa, \mu_z) \tag{10}$$

where f_r^-, f_r^+, and f_r^0 are the resonant frequencies of the HE_{111}^-, HE_{111}^+, and H_{011} modes, respectively.

Equations (8) and (9) were arranged in such a way that function F_1 depends predominantly on κ and function F_2 depends predominantly on μ. This arrangement improves the iterative process used for the solution of the above system of equations. We have used the same computer program used in the previous section of this paper for the computations of F_1, F_2, and F_3.

The imaginary parts of the permeability tensor components were found after computations of their real parts as

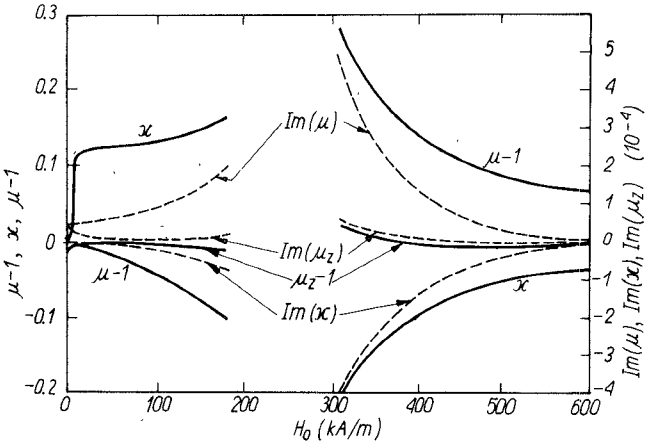

Fig. 10. Permeability tensor components for yttrium-iron-garnet resonators versus external magnetic field intensity computed on the ground of experiments presented in Fig. 9. $\epsilon=14.15$, $\tan\delta_\epsilon=1.9\times10^{-4}$.

solutions of the following system of equations:

$$\begin{aligned}(Q^-)^{-1} = (Q_c^-)^{-1} &+ p_\epsilon^- \operatorname{Im}(\epsilon)/\epsilon + p_{\epsilon z}^- \operatorname{Im}(\epsilon_z)/\epsilon_z \\ &+ p_\mu^- \operatorname{Im}(\mu)/\mu \\ &+ p_\kappa^- \operatorname{Im}(\kappa)/\kappa + p_{\mu z}^- \operatorname{Im}(\mu_z)/\mu_z \end{aligned} \tag{11}$$

$$\begin{aligned}(Q^+)^{-1} = (Q_c^+)^{-1} &+ p_\epsilon^+ \operatorname{Im}(\epsilon)/\epsilon + p_{\epsilon z}^+ \operatorname{Im}(\epsilon_z)/\epsilon_z \\ &+ p_\mu^+ \operatorname{Im}(\mu)/\mu \\ &+ p_\kappa^+ \operatorname{Im}(\kappa)/\kappa + p_{\mu z}^+ \operatorname{Im}(\mu_z)/\mu_z \end{aligned} \tag{12}$$

$$\begin{aligned}(Q^0)^{-1} = (Q_c^0)^{-1} &+ p_\epsilon^0 \operatorname{Im}(\epsilon)/\epsilon + p_{\epsilon z}^0 \operatorname{Im}(\epsilon_z)/\epsilon_z \\ &+ p_\mu^0 \operatorname{Im}(\mu)/\mu \\ &+ p_\kappa^0 \operatorname{Im}(\kappa)/\kappa + p_{\mu z}^0 \operatorname{Im}(\mu_z)/\mu_z. \end{aligned} \tag{13}$$

Here Q^-, Q^+, and Q^0 are the unloaded Q factors for the HE_{111}^-, HE_{111}^+, and H_{011} mode, respectively; Q_c^-, Q_c^+, and Q_c^0 are the Q factors depending on conductor losses for the HE_{111}^-, HE_{111}^+, and H_{011} mode, respectively; and p_x^-, p_x^+, and p_x^0 are the electric or the magnetic energy filling factors computed as follows [9]:

$$p_x^- = 2|\partial f_r^-/\partial x|x/f_r^-$$

$$p_x^+ = 2|\partial f_r^+/\partial x|x/f_r^+$$

$$p_x^0 = 2|\partial f_r^0/\partial x|x/f_r^0$$

where x denotes ϵ, ϵ_z, μ, κ, or μ_z, respectively.

To avoid rather cumbersome Q_c factor computations the following simplifications have been employed:

1) The value of the unloaded Q factor for the HE_{111} mode (with no field applied) was measured and the value of Q_c for this mode was evaluated from (11) or (12) assuming that the material properties for the HE_{111} and the H_{011} mode resonators were the same.
2) It was assumed that when the magnetic field is applied all Q_c factors change their values only due to the change of the surface resistance value. (It is well known that the surface resistance is proportional to the square root of frequency.)

TABLE III
MEASUREMENTS OF PERMITTIVITY TENSOR COMPONENTS OF SINGLE-CRYSTAL QUARTZ

Mode	H_{011}	HE_{211}	E_{011}
Resonant frequency (MHz)	8540.5	8663.4	8718.5
Parameter to be measured	$\epsilon = 4.43$	$\epsilon_z = 4.59$	$\epsilon_z = 4.58$

$h = L = 9.40$; $a = 18.85$ mm; $R_c = 70$ mm.

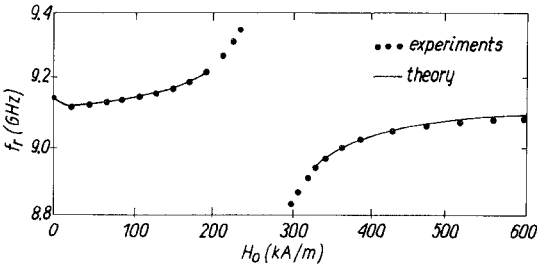

Fig. 11. $H_{01\delta}$-mode resonant frequency of the cylindrical yttrium-iron-garnet resonator having $h = 8.38$ mm, $a = 4.19$ mm, $L = 10.00$ mm, and $\epsilon = 14.15$ versus external magnetic field intensity. Permeability tensor components are taken to be the same as in Fig. 10.

The results of the computations of permeability tensor components are presented in Fig. 10. We remark that the method described here is particularly useful for measurements of low-loss ferrites.

Measurements of permittivity tensor components of single-crystal quartz were performed using only one cylindrical resonator operating on different modes (components of the permittivity tensor of quartz are constants up to infrared frequencies [10] so we do not need to measure them at fixed frequency). The manufacturer ensured that the z axis of the resonator cylinder is oriented along the anisotropy axis of the crystal with an accuracy better than 1°. The resonant frequencies for the first few modes of the resonator have been measured in the Courtney holder. The results of measurements and computations of permittivity tensor components are presented in Table III. First we found the ϵ component of the permittivity tensor solving the transcedental equation for the H_{011} mode (it is exactly the same as for the isotropic H_{011} mode resonator). Then we found the ϵ_z component both from the E_{011} mode frequency and from the HE_{211} mode frequency. The ϵ_z value was found graphically with the aid of the computer program described in the previous section. The values of ϵ and ϵ_z obtained here (Table III) agree to within 0.5 percent with the results obtained by Wolff and Schwab [10].

In our last experiment we measured the resonant frequencies of an $H_{01\delta}$ mode resonator made of yttrium-iron-garnet ferrite versus the external magnetic field intensity. We used the same resonator as in our first experiment but the distance between conducting plates was made greater ($L = 10$ mm) than the height of the ferrite. The experimental results are presented in Fig. 11. We also computed the $H_{01\delta}$ mode resonant frequencies of the resonator for the frequency ranges where the permeability tensor components were known. The results of the computations are shown in Fig. 11 in solid lines. The agreement between theory and experiment confirms the validity of the theory for more complicated resonant structures as well.

V. CONCLUSIONS

In this paper a numerical method was discussed which makes it possible to understand the influence of uniaxial anisotropy and gyrotropy on the resonant frequencies of cylindrical anisotropic resonators. It has also been shown how to use such resonators for measurements of permittivity or permeability tensor components. We note that the computer program used for our computations can easily be modified for analysis of more complicated resonant structures having rotational symmetry (e.g. a ferrite resonator on microstrip line).

APPENDIX
BASIS FUNCTIONS FOR CYLINDRICAL CAVITY

1) Magnetic-Type Rotational Basis Functions:

$$\vec{E}_i^{0H} = -\operatorname{curl}\left(\psi_i^H \vec{i}_z\right)$$

$$\vec{H}_i^{0H} = \left(j\omega_i^{0H}\mu_0\right)^{-1} \operatorname{curl}\operatorname{curl}\left(\psi_i^H \vec{i}_z\right)$$

$$\psi_i^H = A_i J_m\left(k_\rho^H \rho\right)\sin\left(k_z^H z\right)\exp\left(\pm jm\phi\right)$$

$$k_\rho^H = u'_{mn}/a \qquad k_z^H = p\pi/L, \qquad p = 1,2,3,\cdots$$

$$\omega_i^{0H} = c\sqrt{\left(k_\rho^H\right)^2 + \left(k_z^H\right)^2},$$

i being any permutation of (m, n, p).

2) Electric-Type Rotational Basis Functions:

$$\vec{E}_i^{0e} = \left(j\omega_i^{0E}\epsilon_0\right)^{-1} \operatorname{curl}\operatorname{curl}\left(\psi_i^E \vec{i}_z\right)$$

$$\vec{H}_i^{0E} = \operatorname{curl}\left(\psi_i^E \vec{i}_z\right)$$

$$\psi_i^E = B_i J_m\left(k_\rho^E \rho\right)\cos\left(k_z^E z\right)\exp\left(\pm jm\phi\right)$$

$$k_\rho^E = u_{mn}/a \qquad k_z^E = p\pi/L, \qquad p = 0,1,2,\cdots$$

$$\omega_i^{0E} = c\sqrt{\left(k_\rho^E\right)^2 + \left(k_z^E\right)^2}.$$

3) Potential Electric-Type Basis Functions:

$$\vec{F}_i^0 = \operatorname{grad}\phi_i^E$$

$$\phi_i^E = C_i J_m\left(k_\rho^E \rho\right)\sin\left(k_z^H z\right)\exp\left(\pm jm\phi\right).$$

4) Potential Magnetic-Type Basis Functions:

$$\vec{G}_i^0 = \operatorname{grad}\phi_i^H$$

$$\phi_i^H = D_i J_m\left(k_\rho^H \rho\right)\sin\left(k_z^E z\right)\exp\left(\pm jm\phi\right).$$

Here A_i, B_i, C_i, and D_i are amplitudes chosen so as to obtain orthonormal sets of basis functions; i.e. the functions are subjected to the following conditions:

$$\langle \epsilon_0 \vec{E}_i^0, \vec{E}_i^0 \rangle = 1 \qquad \langle \mu_0 \vec{H}_i^0, \vec{H}_i^0 \rangle = 1$$

$$\langle \epsilon_0 \vec{F}_i^0, \vec{F}_i^0 \rangle = 1 \qquad \langle \mu_0 \vec{G}_i^0, \vec{G}_i^0 \rangle = 1.$$

REFERENCES

[1] R. F. Harrington, *Field Computations by Moment Methods*. New York: Macmillan, 1968, ch. 9.

[2] V. V. Nikolskij, *Variational Methods for Electrodynamic Problems*. Moscow: Science, 1967, ch. 2.

[3] M. L. Kales, "Modes in waveguides containing ferrites," *J. Appl. Phys.*, vol. 24, pp. 604–608, May 1953.

[4] R. A. Waldron, "Electromagnetic wave propagation in cylindrical waveguide containing gyromagnetic media," *J. Brit. Inst. Radio Eng.*, vol. 18, pp. 597–610, pp. 671–690, pp. 733–746, 1958.

[5] H. E. Bussey and L. A. Steinert, "Exact solution for a gyromagnetic sample and measurements on a ferrite," *IRE Trans. Microwave Theory Tech.*, vol. MTT-6, pp. 72–76, Jan. 1958.

[6] A. G. Gurevich, *Ferrites at Microwave Frequencies*. New York: Consultants Bureau Enterprises, Inc., 1963, ch. 5.

[7] J. Krupka, "An accurate method of permittivity and loss tangent measurements of low loss dielectrics using $TE_{01\delta}$ dielectric resonators," in *Proc. 5th Int. Conf. Dielectric Materials, Measurements and Applications* (Canterbury, UK) 27–30 June 1988, pp. 322–325.

[8] W. E. Courtney, "Analysis and evaluation of a method of measuring the complex permittivity and permeability of microwave insulators," *IEEE Trans. Microwave Theory Tech.*, vol. MTT-18, pp. 476–485, Aug. 1970.

[9] J. Krupka, "Properties of shielded cylindrical quasi-TE_{0mn}-mode dielectric resonators," *IEEE Trans. Microwave Theory Tech.*, vol. 36, pp. 774–779, Apr. 1988.

[10] I. Wolff and N. Schwab, *Messing der Dielektrizitätszahl anizotroper dielektrischer Materialien im Mikrowellenbereich*. Opladen: Westdeutscher Verlag, 1980.

✠

Jerzy Krupka was born in Cracow, Poland, in 1949. He received the M.Sc. (honors) and Ph.D. degrees from the Warsaw University of Technology in 1973 and 1977, respectively.

Since 1973 he has been associated with the Institute of Microelectronics and Optoelectronics, Warsaw University of Technology, where he is now an Assistant Professor. While on leave during the academic year 1981/1982 he was a Lecturer in the Physics Department, University of Jos, Nigeria. His current research interests are concerned with numerical methods in electromagnetic field theory and measurements of dielectric and magnetic material properties at microwave frequencies.